Progress In Electromagnetics Research C, Vol. 116, 171–180, 2021

Efficient Diplexer with High Selectivity and Low Insertion Loss Based on SOLR and DGS for WIMAX

Asmaa E. Ammar[1, *], Nessim M. Mahmoud[1], Mahmoud A. Attia[1], and Amr H. Hussein[1, 2]

Abstract—In this paper, a highly efficient microstrip diplexer with low insertion loss, high selectivity, and high isolation is introduced. The proposed diplexer employed two compact size coupled squared open-loop resonator (SOLR) based band pass filters (BPFs). Firstly, a matching network is utilized to ensure that the two BPFs and the antenna load are properly matched. This is accomplished by connecting the two BPFs and the antenna with a conventional T-junction that acts as a combining circuit, resulting in good isolation between the uplink and downlink BPFs. As a second step, a defected ground structure (DGS) is used to improve the overall filter response in terms of insertion loss and isolation without affecting the diplexer selectivity. Based on this structure, the proposed diplexer has two resonance frequencies of 2.5 GHz and 2.8 GHz. The structure provides good insertion losses of about 1.6 and 1.3 dB for the two channels, respectively with fractional bandwidth of 2.8% at 2.5 GHz and 3.2% at 2.8 GHz. The measured isolation levels are 70 dB and 50 dB for 2.5 GHz and 2.8 GHz, respectively. The proposed diplexer is useful for several wireless communication applications such as WiMAX. The good agreements between simulated and measured results verified the practical validation of the proposed diplexer.

1. INTRODUCTION

Diplexers are essential components used to minimize the number of antennas in modern high-speed wireless applications such as code-division-multiple-access (CDMA), global system for mobile (GSM), and universal mobile telecommunications system-wide band CDMA (UMTS-WCDMA) [1]. In general, diplexers are made up of two filters for uplink and downlink channels that are connected by a matching/combining network. The matching network is used to guarantee that both filters and the antenna are properly matched. The combining network, on the other hand, is employed to ensure adequate isolation between the uplink and downlink filters. The most popular approach for realizing a diplexer is to combine two band pass filters (BPFs) through a three-terminal matching network [2]. Nevertheless, designing a matching network that can offer excellent transmission in one passband while also providing high attenuation in the other passband is a challenging task. The T-junction impedance matching network has been frequently utilized in diplexers as a three-port matching network. Despite its large size, the dimensions of the T-junction must be carefully selected [3, 4].

Many studies have recently been undertaken to develop a high-performance electrical diplexer having a compact size, low insertion loss (IL), excellent frequency selectivity, wide stopband, and high isolation. The distributed coupling feeding line was used to design a microstrip diplexer with reasonably low insertion loss and high isolation; however, it has poor frequency selectivity. The interdigital cells introduced in [5] have been used to enhance the diplexer IL; however, it also has poor

Received 1 September 2021, Accepted 22 October 2021, Scheduled 5 November 2021

* Corresponding author: Nessim M. Mahmoud (eng.nessim@gmail.com).

[1] Electronics and Electrical Communications Engineering Department, Faculty of Engineering, Tanta University, Tanta 31527, Egypt.

[2] Electronics and Communications Engineering Department, High Institute of Engineering and Technology, New Damietta, Egypt.

frequency selectivity. To minimize the diplexer size, stepped impedance resonator (SIR) and dual-mode resonator have been utilized as common resonators in [6], but the isolation seemed difficult to control. In [7], the diplexer designs based on left-handed/right-handed (LH/RH) resonators have been introduced; nevertheless, they suffer from high return loss and low isolation. In [8], a compact size diplexer using composite right/left handed (CRLH) transmission line resonators has been presented; however, the isolation needs further improvement. A multilayer structure has been utilized to build a compact size diplexer in [9]. Nerveless, the multilayer structure complicates the circuit integration and processing. In [10], a substrate-integrated-waveguide (SIW) based diplexer of high isolation using dual mode resonators has been introduced; however, it still suffers from large size and high insertion loss. Recently, defected ground structures (DGS) have been developed to enhance the properties of various microwave devices, including filters [11], duplexers [12], couplers [13], and antennas [14].

In this paper, a new design topology for a microstrip diplexer having high isolation and low insertion loss is introduced. The proposed diplexer is made up of two compact size BPFs that are made up of coupled SOLRs. The two BPFs are matched to the antenna through a T-junction that functions as a combining circuit, resulting in good isolation between the uplink and downlink BPFs. Firstly, a high selectivity BPF is designed for operation at 2.5 GHz. The other BPF is then designed for operation at 2.8 GHz and is connected with the first one through a T-junction to form the proposed microstrip diplexer. Finally, four large DGS cells were etched under the feed lines of the SOLRs to improve the external quality factor, which in turn significantly improve the filters insertion loss and isolation without affecting the bandwidth.

2. PROPOSED DIPLEXER

In this section, a new design for a three-terminal diplexer, which has two resonance frequencies of 2.5 GHz and 2.8 GHz is proposed. The coupled SOLR is utilized in this diplexer to build the required band pass filters since SOLR provides compact size components, which are of great importance in modern wireless communication systems [15]. The proposed diplexer is designed and simulated on a Rogers TMM4 substrate having a thickness $h = 1.52$ mm and a relative dielectric constant $\varepsilon_r = 4.5$. The simulations are carried out using the computer simulation technology (CST) microwave studio software package (CST-MWS-2019). The diplexer design procedure followed three steps:

(i) Design of the proposed SOLR based BPFs.
(ii) Design of the initial structure of the proposed microstrip diplexer.
(iii) Performance enhancement of the proposed diplexer using DGS technique.

2.1. The Proposed SOLR Based BPF

Because of its tiny dimensions about $(\lambda_g/4) \times (\lambda_g/4)$, where λ_g is the guided wavelength at the mid band frequency [14–16], the microstrip SOLR is one of the most basic and commonly utilized structures for filter construction. At the resonance frequency, both OLRs have the highest electric field density and the highest magnetic field density on the side with the open gap and the opposite side, respectively. By adjusting the direction of orientation of each pair of resonators, three types of couplings, electric-coupling, magnetic-coupling, and mixed-coupling can be produced as illustrated in Fig. 1. In the case of electric-coupling, the pair of resonators interact mainly through their electric fields as shown in Fig. 1(a). At coupling, the two resonators resonate together at two distinct resonance frequencies f_e and f_m, which differ from their fundamental resonance frequency f_0. The difference between the fundamental frequency and the two generated frequencies relies on the resonators' coupling. The electric-coupling resonance f_e and magnetic-coupling resonance f_m are given by:

$$f_e = \frac{1}{2\pi\sqrt{L\,(C + C_m)}} \tag{1}$$

$$f_m = \frac{1}{2\pi\sqrt{L\,(C - C_m)}} \tag{2}$$

where L and C represent the inductance and capacitance per unit length of each of OLRs, respectively, and C_m represents the mutual capacitance owing to electric coupling.

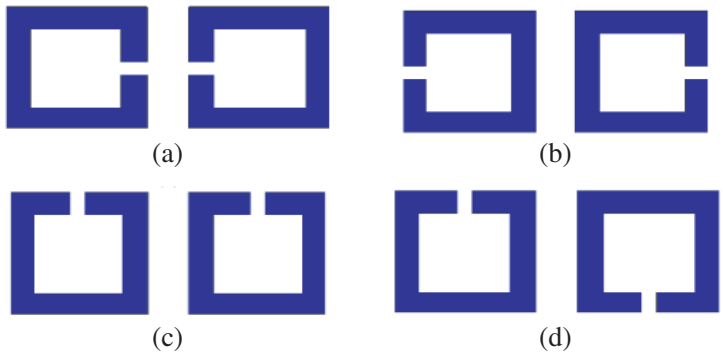

Figure 1. Typical coupling structures of coupled OLRs with (a) electric-coupling, (b) magnetic-coupling, (c), and (d) mixed-coupling.

Firstly, the conventional coupled SOLR is used to design the first BPF. This BPF is made up of two electrically coupled SOLRs, each with a total length about $(\lambda_g/2)$ at the center frequency of 2.5 GHz. The SOLR has a side length, $L_r = 9.5$ mm and a trace width, $W = 1.5$ mm. The coupling strength between the SOLRs is controlled by the separation gap g, resulting in bandwidth and insertion loss (IL) control, as shown in Fig. 2. The internal capacitance of each resonator is controlled by the gap width $S = 1.3$ mm. When the gap width S decreases, the capacitance increases, and the internal resonator size decreases. The BPF is designed and simulated on a Rogers TMM4 substrate with thickness $h = 1.52$ mm and $\varepsilon_r = 4.5$.

The feed line positions (ports 1 and 2) should be carefully adjusted to guarantee that the resonance modes are stimulated. The external quality factor is particularly high when the tapped feed line is situated in the middle of the resonator because the resonator cannot be stimulated at that position [16].

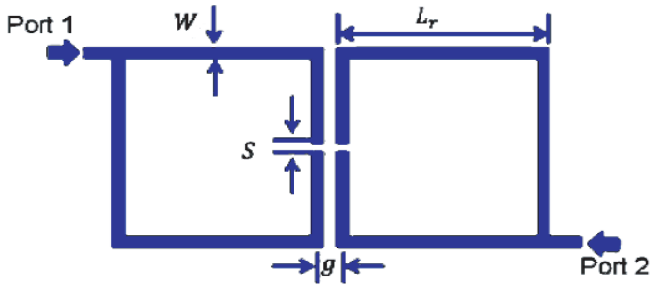

Figure 2. The configuration of the conventional coupled SOLR-based BPF.

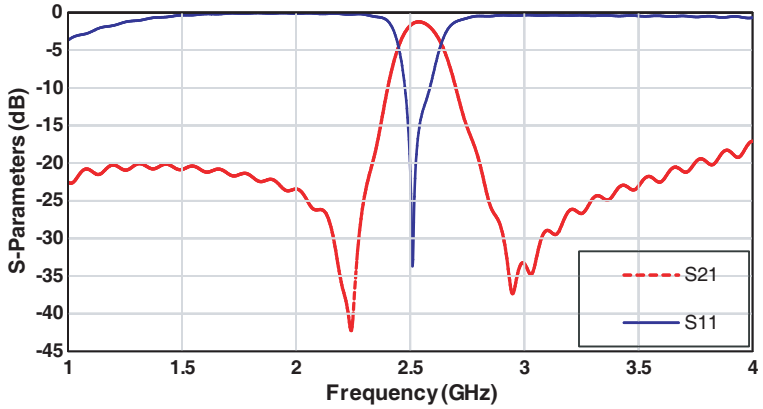

Figure 3. Simulated scattering parameters of the proposed BPF.

The use of asymmetric feeding and electric coupling improves the filter stopband characteristics by introducing two transmission zeros close to and on the opposite sides of the passband and, hence, the BPF selectivity is significantly increased.

Figure 3 displays the simulation results of the proposed BPF using the CST-MWS simulator. The band pass filter has a center frequency of 2.5 GHz, a fractional bandwidth of 8%, a return loss of 35 dB, and an insertion loss of 1%. Furthermore, the band pass filter exhibits two transmission zeros at the passband boundary at 2.2 GHz and 2.9 GHz.

2.2. Initial Structure of the Proposed Microstrip Diplexer

In this section, the initial configuration of the proposed diplexer is introduced to identify the initial performance characteristics. A microstrip diplexer can be designed using a variety of filter combinations, such as low pass and high pass filters, or band pass and band stop filters [17]. The proposed diplexer configuration is based on the use of the two SOLR-based BPFs described in Section 2.1. The proposed diplexer's construction begins with the design of two SOLR-based BPFs operating at 2.5 GHz and 2.8 GHz for transmitting (Tx) and receiving (Rx), respectively. The two filters are connected to each other through a T-junction to feed the Tx/Rx antenna port. The isolation between the transmitting and receiving channels is dependent on the appropriate choice of the width and length of the T-junction branches. Fig. 4 illustrates the proposed diplexer layout, which includes two SOLRs-based PBFs with the dimensions listed in Table 1.

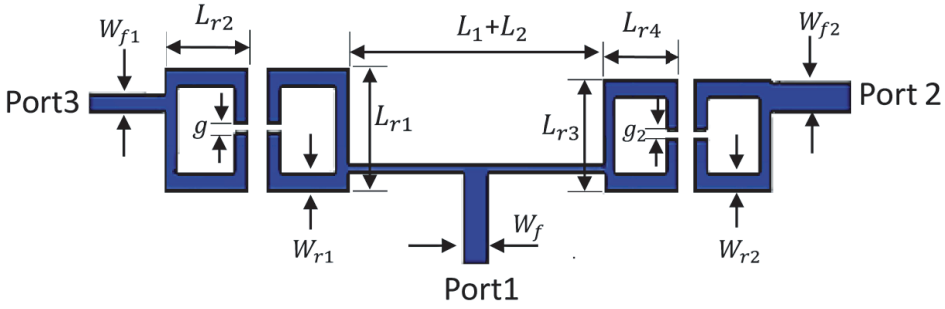

Figure 4. The initial layout of the proposed diplexer.

Table 1. Dimensions in (mm) of the initially proposed diplexer.

W_{f1}	L_{r1}	L_{r2}	g	g_2	L_1	L_2
1.4	11	9.7	2.15	1.9	15	15
W_f	W_{f2}	L_{r3}	L_{r4}	W_{r1}	W_{r2}	
2.8	2.8	9.7	9	1.5	1.5	

The lower-band transmitting BPF is designed with its two transmission zeros such that one of them is located in the passband of the higher-band receiving BPF. While the higher-band receiving BPF has a transmission zero in the passband of the transmitting BPF. Based on this concept, the lower- and upper-passbands are well isolated which improves their mutual interference and explains the good isolation between the two channels. Fig. 5 shows the optimized simulation results of the three scattering parameters $|S_{11}|$, $|S_{21}|$, and $|S_{31}|$ versus frequency of the proposed diplexer and also clarifies the success of the proposed isolation concept where around 60 dB isolation is achieved for the two bands. By analyzing the results, it is found that the insertion losses of the two BPFs are 1.8 dB and 1.4 dB at 2.5 GHz and 2.8 GHz, respectively with desired 3 dB bandwidths of 0.08 GHz for the 2.5 GHz band and 0.09 GHz for the 2.8 GHz band. In other words, the realized fractional bandwidths are 3.2% and 3.21% for 2.5 GHz and 2.8 GHz bands, respectively.

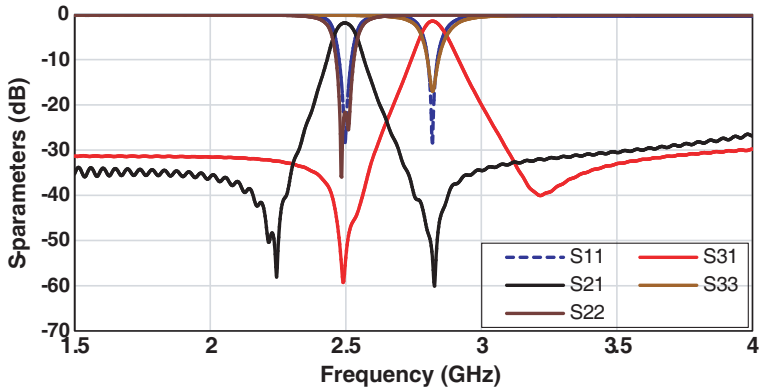

Figure 5. Simulated scattering parameters of the initially proposed diplexer.

However, these results reveal that the initial design of the diplexer has certain shortcomings, such as high insertion loss, poor selectivity (broad bandwidth), and good isolation, which may be improved further. These issues are resolved utilizing DGS, as explained in the next section.

2.3. Final Configuration of the Proposed Microstrip Diplexer

The diplexer insertion loss can be improved by using inter-digital cells as in [5]; however, it suffers from poor frequency selectivity. In this section, the DGSs are suggested to improve the performance of the diplexer in terms of isolation and insertion loss. As shown in Fig. 6, four large DGS cells are etched at the ground plane beneath each SOLR. As a result, the etched DGSs alter the distribution of the electric field between the resonators lines and the ground plane such that the effective transverse height between the ground plane and the resonator is virtually increased, which reduces the line capacitance per unit length [18]. Accordingly, the amount of power coupled to the ground plane is reduced while the amount of external power coupled to the resonators from the feeding circuit is increased, which leads to an improvement in the external quality factor of the filter. In addition, the DGS cell and transmission line above the DGS can be modeled as inductors, which improves the diplexer matching. Furthermore, the magnetic current coupled through the DGSs increases, improving the insertion loss of the filter without altering the diplexer bandwidth. The optimized dimensions of the diplexer are listed in Table 2.

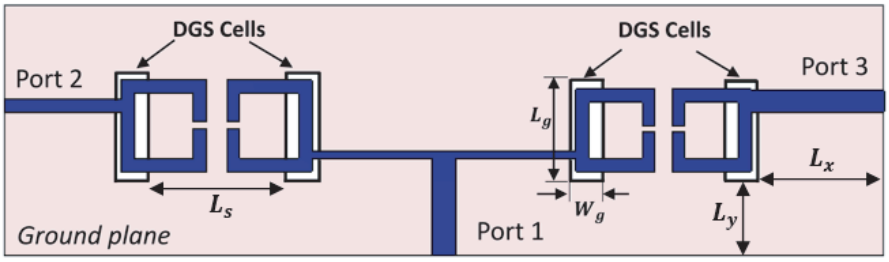

Figure 6. The final configuration of the proposed diplexer using DGS.

Table 2. Dimensions in (mm) of the proposed diplexer after adding DGS.

W_{f1}	L_{r1}	L_{r2}	g	g_2	L_1	L_2	L_x	L_s
1.4	10.4	9.7	2.3	1.9	15	15	12.8	17.7
W_f	W_{f2}	L_{r3}	L_{r4}	W_{r1}	W_g	L_g	L_y	
2.8	2.4	9.4	9	1.5	2.5	10.6	8.95	

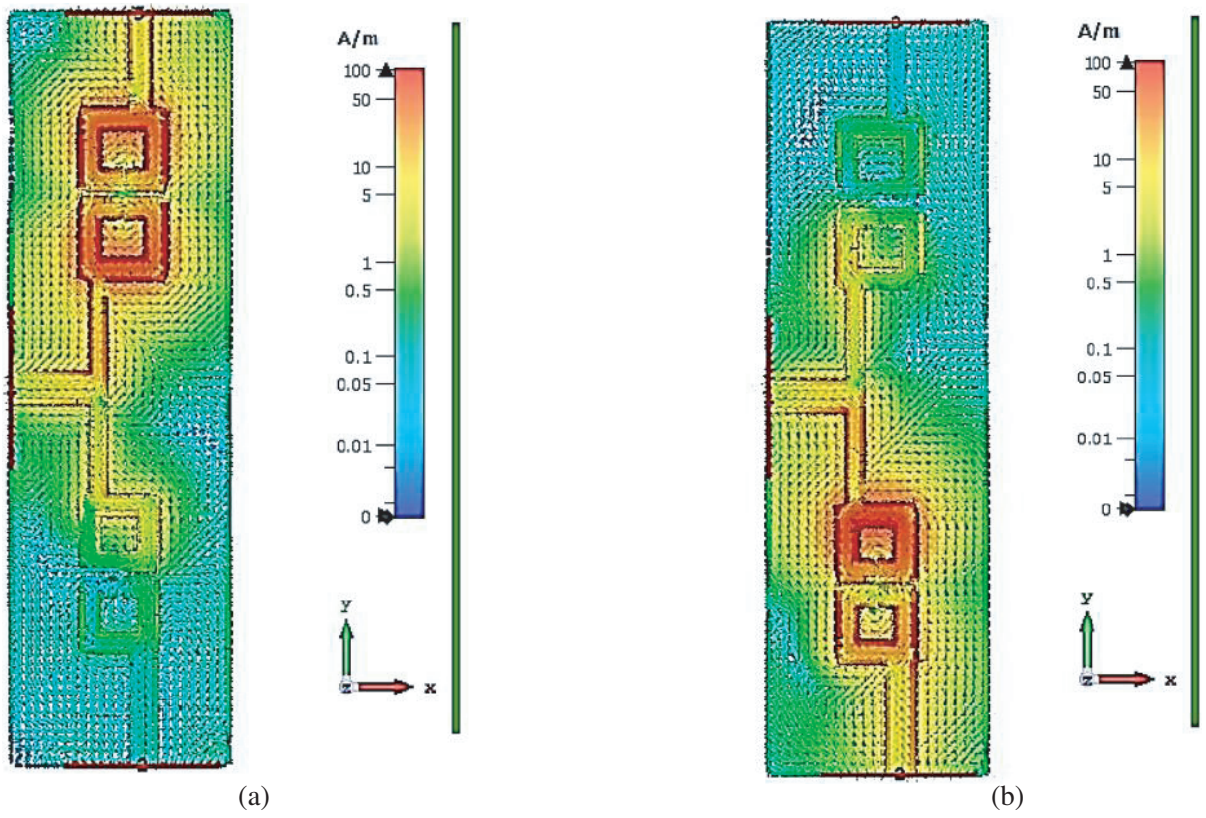

Figure 7. Surface currents of the proposed diplexer at: (a) $f_t = 2.5\,\text{GHz}$ and (b) $f_r = 2.8\,\text{GHz}$.

Figure 7 depicts the distributions of the electric field of the proposed diplexer at the lower and upper passbands. When the diplexer is operating at the lower passband (2.5 GHz), the high current density is concentrated mostly in the lower passband channel, while the upper passband channel (2.8 GHz) is considered as an open circuit as shown in Fig. 7(a). Contrarily, when the diplexer is operating at the upper passband (2.8 GHz), the high current density is located at the higher passband channel, whereas the lower passband channel (2.5 GHz) is considered as an open circuit as shown in Fig. 7(b).

Figure 8 shows the simulated S-parameters of the proposed diplexer employing DGSs. The proposed diplexer has improved insertion losses from 1.8 dB and 1.4 dB to 1.2 dB and 1.3 dB for the 2.5 GHz and

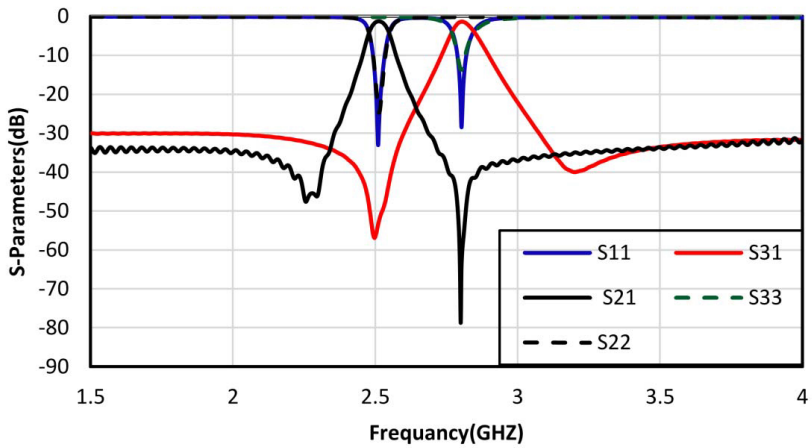

Figure 8. Simulated scattering parameters of the proposed diplexer with DGS.

2.8 GHz bands, respectively, while the selectivity or FBW is increased from 3.2% to 2.8% for both bands. The isolation after introducing the DGSs is 53.5 dB and 63 dB for 2.5 GHz and 2.8 GHz, respectively.

3. FABRICATION AND MEASUREMENTS

The proposed diplexer prototype is fabricated on a Rogers TMM4 substrate with dielectric constant $\varepsilon_r = 4.5$ and thickness $h = 1.52\,\text{mm}$ as shown in Fig. 9. The diplexer size is $(100 \times 28.5)\,\text{mm}^2$. The scattering parameters of the fabricated diplexer were measured using the Rohde & Schwarz ZVL20 Network Analyzer. Fig. 10 represents the simulated and measured results denoted by solid and dashed lines, respectively, which illustrates that the fractional bandwidth is 2.8% and 3.2% for the Tx channel and Rx channel, respectively. The measured insertion loss is 1.6 dB at 2.5 GHz and 1.3 dB at 2.8 GHz.

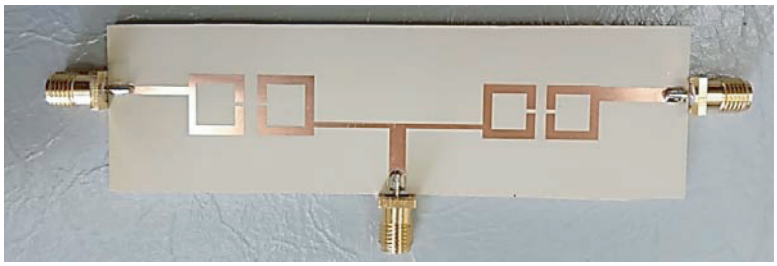

(a)

(b)

Figure 9. Photograph of the fabricated diplexer. (a) Top view. (b) Bottom view.

Table 3. Comparison of the proposed diplexer with the most related works.

Diplexer	Frequency (GHz)	Fractional bandwidth (%)	Insertion loss (dB)	Isolation (dB)	Size λ_g^2
This work	**2.5/2.8**	**2.8/3.2**	**1.6/1.3**	**70/50**	**0.32**
Ref. [2] (2009)	1.9/2.1	3.07/2.8	3/3	> 40	NA
Ref. [20] (2015)	2.4/3.42	7.2/7.2	1.43/1.56	> 40	0.27
Ref. [19] (2018)	2.95, 4.92	12.8/9.3	1.47/ 1.43	> 40	0.0522
Ref. [21] (2018)	2.2/2.6	4.55/5	1.6/1	> 40	NA
Ref. [10] (2020)	8.04/9.07	4.23/4.19	2.35/2.33	49.53	4.6
Ref. [22] (2021)	4.3/8.75	50/51.4	2.3/3.0	25	0.13
Ref. [23] (2021)	2.1/2.6	4/4	1.4/1.3	> 40	0.59

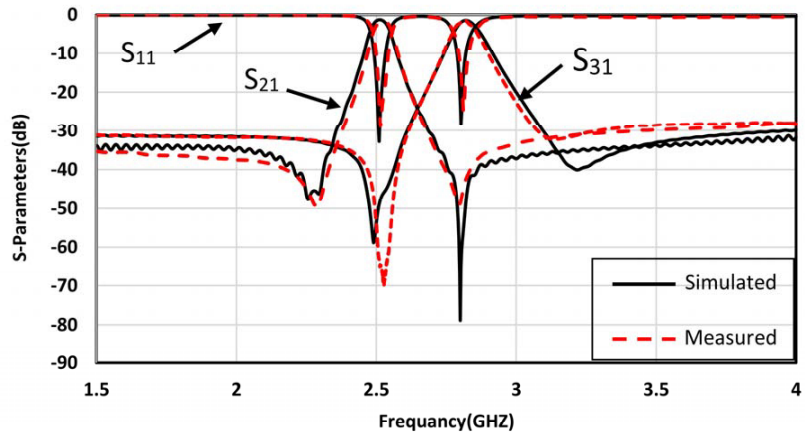

(a)

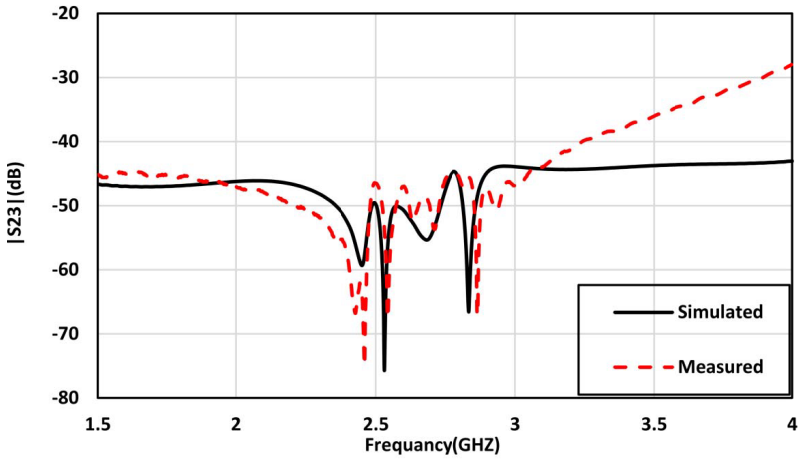

(b)

Figure 10. Measured scattering parameters of the fabricated diplexer. (a) $|S_{11}|$, $|S_{21}|$, and $|S_{31}|$. (b) The isolation $|S_{23}|$.

The isolation is 70 dB and 50 dB for 2.5 GHz and 2.8 GHz, respectively. Generally, when TX- and RX-band frequencies are in close vicinity, the isolation becomes a critical issue in a diplexer. Based on the introduced measurements, the proposed diplexer presented in this paper provides significant isolation. The comparison between simulated and measured results revealed good agreement.

4. COMPARISON WITH RELATED WORK

In this section, a comparison is performed between the proposed diplexer's results and the related work to demonstrate the benefits of the proposed diplexer, as shown in Table 3. The fabricated diplexer has the highest selectivity (lowest FBW) so far, except for [2], which has almost the same bandwidth; nevertheless, the proposed diplexer is superior in terms of lower insertion loss and better isolation. Even though the proposed diplexer has a somewhat larger area than [19–22], the fabricated diplexer has significantly higher selectivity and better isolation. Finally, compared to [23], the insertion loss is almost the same. The designs in [22, 23], on the other hand, have a greater fractional bandwidth and lower isolation. This comparison shows that the proposed diplexer outperforms the competitors in terms of the tradeoff between size and performance characteristics.

5. CONCLUSION

In this paper, a highly efficient design for a microstrip diplexer with high selectivity, high isolation, and low insertion loss based on the utilization of two SOLR-based BPFs is introduced. The diplexer utilized T-junction as a combining circuit to connect the two BPFs, which in turn improved the isolation between the transmitting and receiving bands of the diplexer. Finally, DGS cells were used under the feeding lines to improve the external quality factor, which in turn improved the performance of the diplexer in terms of isolation (70 dB/50 dB) and insertion loss (1.6 dB/1.3 dB) without affecting the fractional bandwidth (2.8%/3.2%) for the transmitting and receiving bands, respectively. The scattering parameters of the fabricated diplexer are measured using the Rohde & Schwarz ZVL20 Network Analyzer and are found to highly match the simulation results.

REFERENCES

1. Tang, H. J., W. Hong, J.-X. Chen, G. Q. Luo, and K. Wu, "Development of millimeter-wave planar diplexers based on complementary characters of dual-mode substrate integrated waveguide filters with circular and elliptic cavities," *IEEE Transactions on Microwave Theory and Techniques*, Vol. 55, 776–782, 2007.
2. Konpang, J., "A compact diplexer using square open loop with stepped impedance resonators," *2009 IEEE Radio and Wireless Symposium*, 91–94, 2009.
3. Duan, Q., K. Song, F. Chen, and Y. Fan, "Compact wide-stopband diplexer using dual mode resonators," *Electronics Letters*, Vol. 51, 1085–1087, 2015.
4. Yang, T., P.-L. Chi, and T. Itoh, "High isolation and compact diplexer using the hybrid resonators," *IEEE Microwave and Wireless Components Letters*, Vol. 20, 551–553, 2010.
5. Bui, D., T. Vuong, B. Allard, J. Verdier, and P. Benech, "Compact low-loss microstrip diplexer for RF energy harvesting," *Electronics Letters*, Vol. 53, 552–554, 2017.
6. Guan, X., F. Yang, H. Liu, and L. Zhu, "Compact and high-isolation diplexer using dual-mode stub-loaded resonators," *IEEE Microwave and Wireless Components Letters*, Vol. 24, 385–387, 2014.
7. Xu, K. D., M. Li, Y. Liu, Y. Yang, and Q. H. Liu, "Design of triplexer using E-stub-loaded composite right-/left-handed resonators and quasi-lumped impedance matching network," *IEEE Access*, Vol. 6, 18814–18821, 2018.
8. Li, M., K. D. Xu, J. Ai, and Y. Liu, "Compact diplexer using short stub-loaded composite right/left-handed resonators," *Microwave and Optical Technology Letters*, Vol. 59, 1470–1474, 2017.
9. Hong, J.-S. and M. J. Lancaster, "Couplings of microstrip square open-loop resonators for cross-coupled planar microwave filters," *IEEE Transactions on Microwave Theory and Techniques*, Vol. 44, 2099–2109, 1996.
10. Cheng, F., C. Gu, B. Zhang, Y. Yang, and K. Huang, "High isolation substrate integrated waveguide diplexer with flexible transmission zeros," *IEEE Microwave and Wireless Components Letters*, Vol. 30, 1029–1032, 2020.
11. Mahmoud, N., A. Barakat, M. Nasr, and R. K. Pokharel, "Performance enhancement of 60 GHz CMOS band pass filter employing oxide height virtual increase," *Progress In Electromagnetics Research*, Vol. 77, 125–134, 2019.
12. Hussein, A. H., H. H. Abdullah, M. A. Attia, and A. M. Abada, "S-band compact microstrip full-duplex tx/rx patch antenna with high isolation," *IEEE Antennas and Wireless Propagation Letters*, Vol. 18, 2090–2094, 2019.
13. Sharma, R. Y., T. Chakravarty, S. Bhooshan, and A. B. Bhattacharyya, "Design of a novel 3dB microstrip backward wave coupler using defected ground structure," *Progress In Electromagnetics Research*, Vol. 65, 261–273, 2006.
14. Pandit, S., A. Mohan, P. Ray, and B. Rana, "Compact four-element MIMO antenna using DGS for WLAN Applications," *2018 International Symposium on Antennas and Propagation (ISAP)*, 1–2, 2018.

15. Lee, H., C.-T. M. Wu, and T. Itoh, "Study and analysis of contiguous channel triplexer based on combining method of two filtering circuits using CRLH and RH isolation circuits," *International Journal of Microwave and Wireless Technologies*, Vol. 6, 287–295, 2014.
16. Hong, J.-S. G. and M. J. Lancaster, *Microstrip Filters for RF/Microwave Applications*, Vol. 167, John Wiley & Sons, 2004.
17. Yao, H.-W., A. E. Abdelmonem, J.-F. Liang, X.-P. Liang, K. A. Zaki, and A. Martin, "Wideband waveguide and ridge waveguide T-junctions for diplexer applications," *IEEE Transactions on Microwave Theory and Techniques*, Vol. 41, 2166–2173, 1993.
18. Khandelwal, M. K., B. K. Kanaujia, and S. Kumar, "Defected ground structure: Fundamentals, analysis, and applications in modern wireless trends," *International Journal of Antennas and Propagation*, Vol. 2017, 2017.
19. Li, Q., Y. Zhang, and C. T. M. Wu, "Compact and high-isolation microstrip diplexer using distributed coupling feeding line," *Microwave and Optical Technology Letters*, Vol. 60, 192–196, 2018.
20. Xiao, J.-K., M. Zhu, Y. Li, L. Tian, and J.-G. Ma, "High selective microstrip bandpass filter and diplexer with mixed electromagnetic coupling," *IEEE Microwave and Wireless Components Letters*, Vol. 25, 781–783, 2015.
21. Tizyi, H., F. Riouch, A. Tribak, A. Najid, and A. Mediavilla, "Microstrip diplexer design based on two square open loop bandpass filters for RFID applications," *International Journal of Microwave and Wireless Technologies*, Vol. 10, 412, 2018.
22. Zhang, P., M.-H. Weng, and R.-Y. Yang, "A compact wideband diplexer using stub-loaded square ring resonators," *Electromagnetics*, Vol. 41, 167–184, 2021.
23. Hassan, A. Y., M. F. Hagag, A. A. Abdel Aziz, and M. A. Abdalla, "A compact diplexer using coupled π-CRLH zeroth resonators," *IETE Journal of Research*, 1–8, 2021.